Available online at www.sciencedirect.com

ScienceDirect

Solar Energy 108 (2014) 360–369

SOLAR ENERGY

www.elsevier.com/locate/solener

Theoretical study of the efficiency of CdS/PbS thin film solar cells

H.A. Mohamed *

Physics Department, Faculty of Science, Sohag University, 82524 Sohag, Egypt
Physics Department, Teachers College, King Saud University, 11148 Riyadh, Saudi Arabia

Received 29 November 2013; received in revised form 16 July 2014; accepted 18 July 2014

Communicated by: Associate Editor Takhir M. Razykov

Abstract

This work represents a theoretical analysis of a new type of thin film solar cells with structure glass/ITO/CdS/PbS/AL. The transmission spectrum was calculated based on the multi-reflections effect from all cell layers as well as absorption effect in both ITO and CdS layers. The calculations of spectral internal quantum efficiency were carried out based on the front and back surface recombination of PbS layer. The recombination losses in space-charge region were studied. The effect of thickness of the absorber layer on the calculations of short-circuit current density was studied under illumination condition of AM1.5 solar irradiation. The data of open circuit voltage, maximum voltage, maximum current density, fill factor, output power density and efficiency of CdS/PbS solar cell were estimated from the *J–V* characteristics curve under illumination effect. This study ignored the effect of metallic back contact and thus the incomplete absorption losses (transmission losses) take place at thin absorber layer. The obtained results showed that the 2 μm thickness of the absorber layer is not sufficient to absorb all the transmitted photons from the window layer (CdS) and the selection of theses thin thicknesses of PbS in order to correspond with experimental implementations of these devices. Both the optical and recombination losses lead to decrease the current density by 82% ($J_{SC} = 7.28$ mA/cm^2) at thickness 0.5 μm of PbS and these losses decreased to 67% ($J_{SC} = 16$ mA/cm^2) at thickness 2 μm. The output power density and the cell efficiency increased with increasing the thickness of effective layer. The maximum cell efficiency of 4.13% was obtained at thickness of 2 μm which is considered greater than those obtained experimentally.

Keywords: CdS/PbS thin film solar cell; Transmission spectrum; Internal quantum efficiency; *J–V* curve; Cell efficiency

1. Introduction

Photovoltaic devices usually exploit mid-range band-gap semiconductors which absorb in the visible range of the solar spectrum. CdTe/CdS and CIGS/CdS solar cells are considered the ideal cell of these devices and recently recorded high efficiency of 18.3% and 20% (Mohamed and Hadia, 2013; Green et al., 2013) respectively. However, narrow band-gap semiconductors are of interest for photovoltaic (PV) solar energy conversion as they can absorb the "IR tail" of the solar spectrum, which is not absorbed by commonly used PV materials. The use of such absorbers in semiconductor sensitized solar cells allows the integration of low cost device configurations and broad spectral response, which may also be utilized in IR and near-IR (NIR) photodetectors (Gertman et al., 2014).

Quantum dot-sensitized solar cells (QDSCs) are interesting energy devices because quantum dots (QDs) exhibit some attractive advantages, such as high extinction coefficients, tunable bandgaps simply by controlling the QDs

* Address: Physics Department, Faculty of Science, Sohag University, 82524 Sohag, Egypt.
E-mail address: hussein_abdelhafez2000@yahoo.com

http://dx.doi.org/10.1016/j.solener.2014.07.017
0038-092X/

sizes, low cost and so on (Nozik, 2002; Kramer and Sargent, 2011). The maximum obtained efficiency is in the range 4–7% when ZnO and TiO_2 in their various forms (nanoparticles, nanowires, and bulk thin film) were used as n-type for PbS QDs (Gao et al., 2011; Ip et al., 2012). Bhandari et al., 2013 reported on heterojunction PbS quantum dot (QD) thin film solar cells using RF magnetron sputtered CdS as the n-type window layer. They obtained cell efficiency of 3.3%. The chemical bath deposition method was used to prepare thin film solar cell CdS/PbS with efficiency 1.37 (Obaid et al., 2013b). Moreover, Hernandez-Borja et al., 2011 has reported prototype thin film PbS/CdS solar cells (not QDs) with 1.6% efficiency where both CdS and PbS are deposited by chemical bath method. Lead sulfide (PbS) is an attractive material in that sense (Hernandez-Borja et al., 2011), as it has a high extinction coefficient, band-gap tunability via quantum size effects, and multiple exciton generation which has been demonstrated both for quantum dots and bulk-like PbS thin films (Nair et al., 2011; Velizhanin and Piryatinski, 2011; Sambur et al., 2010; Semonin et al., 2011). Bulk PbS has a narrow band-gap of 0.37–0.41 eV (300 °K) (Smith et al., 2011) and an exciton Bohr radius of 18–20 nm (Wise, 2000).

To our knowledge, the theoretical studies in this type of solar cell are absent in the literatures. This work aims to study the shape and behavior of some quantities such as the internal quantum efficiency, the short-circuit current density and the J–V characteristic curve of thin film photovoltaic solar cell with structure CdS/PbS. Besides, study the dependence of cell parameters such as the efficiency, fill factor, open-circuit voltage and the output power density on the thickness of absorber layer (PbS). The calculations are carried out under at certain parameters such as the electron lifetime, the recombination velocity and the width of space charge region. The optical losses (due to absorption in ITO and CdS and multi-reflections from different layers), the recombination losses at front and back surface of PbS layer and the recombination losses in space-charge region will be taken into consideration. In order to compare the previous experimental results of these devices with the current results, a thin thickness of 0.5–2 μm of the absorber layer will be considered. One should keep in mind that the transmission losses (incomplete absorption) are caused by a thin thickness of the absorber layer and the effect of the metallic back contact will not be taken into consideration. Here, the optical losses simply refer to the absorption losses in ITO and CdS as well as the reflection from all interfaces.

2. Theoretical aspects

2.1. Calculations of transmission spectrum

The schematics structure and band diagram under forward bias of thin film CdS/PbS solar cells is shown in Fig. 1. This cell consists of four layers. The first layer is called front contact which is made from transparent conducting oxide such as indium tin oxide (ITO). The second layer from CdS which is used as n-type semiconductor, this layer is called window layer. The third layer which is called the effective layer is formed from PbS, this layer is used as p-type semiconductor. The last layer is called back contact which is formed from metal that must have high workfunction to make ohmic contact with PbS.

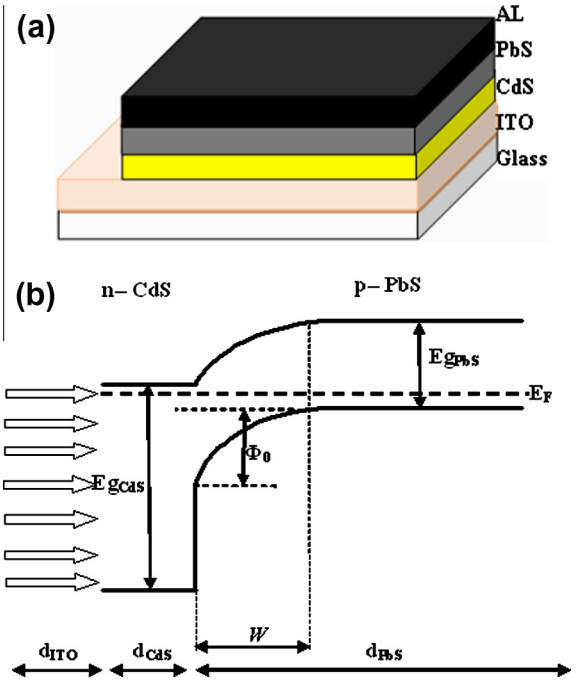

Fig. 1. Schematics of a typical CdS/PbS solar cell structure (a) and schematic of the energy band diagram of CdS/PbS solar cell under forward bias (b).

When the incident light path through CdS/PbS cell, certain part of this radiation is lost due to reflection and absorption effects. The reflection losses is due to reflectivity from different layers of the cell (glass, ITO, CdS and PbS). In addition to reflection losses, absorption losses takes place in ITO and CdS layers. Therefore, these losses will be taken into calculations of the transmitted light that reaches the effective layer (PbS) of the solar cell. To be more accurate, the multi-reflections effect inside CdS/PbS cell will be taken into calculations.

The Fresnel reflection of the normal incident light upon a boundary between two materials of different refractive indices is given by:

$$R_f = \frac{(n_1 - n_2)^2}{(n_1 + n_2)^2} \tag{1}$$

In addition, the Fresnel Power Transmission coefficient is given by:

$$T_f = 1 - R_f = \frac{4n_1 n_2}{(n_1 + n_2)^2} \tag{2}$$

where n_1 and n_2 are the refractive indices of the two media.

The total transmittance for L number of layers can be calculated from:

$$T_R = T_f \prod_{j=2}^{L-1} \frac{T_{j,j+1}}{(1 - R_{j,j-1} R_{j,j+1})} \tag{3}$$

which expands to

$$T_R = 4 \frac{n_1 n_2}{(n_1 + n_2)^2} \prod_{j=2}^{L-1} \frac{4 \frac{n_j n_{j+1}}{(n_j + n_{j+1})^2}}{\left(1 - \frac{(n_j - n_{j-1})^2 (n_j - n_{j+1})^2}{(n_j + n_{j-1})^2 (n_j + n_{j+1})^2}\right)} \tag{4}$$

The transmission coefficient $T(\lambda)$ due to multi-reflections as well as absorption can be written in the form (Mohamed, 2013):

$$T(\lambda) = T_R (e^{-\alpha_1 d_1})(e^{-\alpha_2 d_2}) \tag{5}$$

where α_1, α_2, d_1, d_2 is the absorption coefficient and thickness of ITO and CdS layers, respectively.

The absorption coefficient is calculated from:

$$\alpha(\lambda) = \frac{4\pi}{\lambda} k(\lambda) \tag{6}$$

where k is the extinction coefficient of the used material.

2.2. Calculations of absorptive capacity of PbS

The thickness of absorber layer has a significant effect of the capacity of it to absorb the incident solar radiation. Recently, Kosyachenko et al. (2013) studied the dependence of the absorptivity of solar radiation power on the thickness of absorber layer of CdS/CdTe solar cell. The expression for the integrated (rather than at a certain wavelength) absorptivity of solar radiation in the absorber layer with a thickness d can be represented as:

$$A_\Phi(d) = \frac{\sum_i T(\lambda) \Phi_i [1 - \exp(-\alpha d) \Delta\lambda_i}{\sum_i T(\lambda) \Phi_i \Delta\lambda_i} \tag{7}$$

where Φ_i is the spectral power density (mW cm^{-2} μm^{-1}) at wavelength λ_i and $\Delta\lambda_i$ is the interval between the two neighboring values of wavelength. The current calculations of absorptivity ignore the effect of the metallic back contact.

2.3. Calculations of internal quantum efficiency

The internal quantum efficiency (η_{int}) of a solar cell includes the drift (η_{drift}) and diffusion components (η_{dif}) of quantum efficiency.

The drift component, which takes into account the front surface recombination losses due to recombination at the interface of CdS with PbS, is governed by the following expression (Kosyachenko et al., 2009):

$$\eta_{\text{drift}} = \frac{1 + \frac{S}{D_n}\left(\alpha + \frac{2}{W}\frac{\varphi_0 - qv}{kT}\right)^{-1}}{1 + \frac{S}{D_n}\left(\frac{2}{W}\frac{\varphi_o - qv}{kT}\right)^{-1}} - \exp(-\alpha W) \tag{8}$$

where S is the front surface recombination velocity; v is the applied voltage; φ_o is the barrier height; D_n is the diffusion coefficient of electrons related to their mobility μ_n by the Einstein relation $qD_n/kT = \mu_n$; W is the width of the space charge region; α is the absorption coefficient of PbS at a given wavelength, q is the electron charge, k is the Boltzmann constant and T is room temperate.

The diffusion component of the internal quantum efficiency, which takes into account recombination at the back surface of the solar cell, is given by the following expression (Sze and Kwok, 2007; Yang et al., 2008):

$$\eta_{\text{dif}} = \frac{\alpha L_n}{\alpha^2 L_n^2 - 1} \exp(-\alpha W) \times \left\{ \alpha L_n - \frac{\frac{S_b L_n}{D_n}\left[\cosh\left(\frac{d-W}{L_n}\right) - \exp(-\alpha(d-W))\right] + \sinh\left(\frac{d-W}{L_n}\right) + \alpha L_n \exp(-\alpha(d-W))}{\frac{S_b L_n}{D_n}\sinh\left(\frac{d-W}{L_n}\right) + \cosh\left(\frac{d-W}{Ln}\right)} \right\} \tag{9}$$

where $L_n = (\tau_n D_n)^{1/2}$ is the electron diffusion length; τ_n is electron lifetime; S_b is the velocity of recombination at the rear surface of the PbS layer and d is the thickness of the PbS layer.

The dependence of width W of space-charge region (depletion layer) on the concentration of uncompensated acceptors ($N_a - N_d$) is given by:

$$W = \sqrt{\frac{2\varepsilon\varepsilon_0(\varphi_0 - qv)}{q^2(N_a - N_d)}} \tag{10}$$

where ε is the relative permittivity of the semiconductor and ε_0 is the permittivity of free space.

The internal quantum efficiency η_{int} is the sum of drift and diffusion components:

$$\eta_{\text{int}} = \eta_{\text{drift}} + \eta_{\text{dif}} \tag{11}$$

The values of the above parameters (d_1, d_2, $\varphi_o - qv$, D_n, μ_n, τ_n and ε) are listed in Table1.

2.4. Recombination losses in the space-charge region

In addition to front surface recombination losses and recombination at the back surface of the solar cell, there is a probability that the generated electron–hole pairs recombine within the space-charge region (SCR) and cause losses of the photocurrent in the circuit of photovoltaic device. These losses are depending on some parameters

Table 1
The values of the parameters used in this study.

Symbol	Value	Reference
d_1	100 nm	Current work
d_2	100 nm	Current work
$\Phi_0 - qv$	0.7 eV	Current work
D_n	25.8	Current work
μ_n	1000 $cm^2/(V\,S)$	Current work
μ_P	80 $cm^2/(V\,S)$	Current work
τ_n	10^{-9} s	Current work
τ_P	10^{-9} s	Current work
ε	18	Akhtar et al. (2010)

such as: carrier lifetime (τ_n, τ_p), carrier mobility (μ_n, μ_p), the width of SCR (W) and the strength of the electric-field (F).

The mean distance (the electron drift length) that the electron travels during the mean lifetime τ_n along the electric field is determined by the electron mobility μ_n and the electric field strength F:

$$\lambda_n = \mu_n F \tau_n \tag{12}$$

Then, the hole drift length is given by:

$$\lambda_p = \mu_p F \tau_p \tag{13}$$

In the Schottky diode, an electric field is not uniform in the space-charge region, but consideration of the nonuniformity is simplified, since the field strength decreases linearly with the x coordinate. In this case, the field strength F in the expressions (12) and (13) for λ_n and λ_p can be replaced by the average values of F in the sections (0, x) and (x, W) for electrons and holes, respectively (Kosyachenko et al., 2006):

$$F(0,x) = \frac{\Phi_0 - eV}{eW}\left(2 - \frac{x}{W}\right) \tag{14}$$

$$F(x,W) = \frac{\Phi_0 - eV}{eW}\left(1 - \frac{x}{W}\right) \tag{15}$$

The charge collection efficiency is expressed by the known Hecht equation (Hecht, 1932):

$$\eta_c = \frac{\mu_p F(x,W)\tau_p}{W}\left[1 - \exp\left(-\frac{W-x}{\mu_p F(x,W)\tau_p}\right)\right] + \frac{\mu_n F(0,x)\tau_n}{W}\left[1 - \exp\left(-\frac{x}{\mu_n F(0,x)\tau_n}\right)\right] \tag{16}$$

2.5. Calculations of short-circuit current density

The spectral distribution of the photons can be found as $\Phi_i/h\nu$, where Φ_i is the spectral power density ($mW\,cm^{-2}\,\mu m^{-1}$), and $h\nu$ is the photon energy. By using Eqs. (5) and (8)–(11), the short-circuit current density (J_{SC}) can be calculated according to this formula:

$$J_{SC} = q\sum_i T(\lambda)\frac{\varphi_i(\lambda_i)}{h\nu_i}\eta_{int}(\lambda_i)\Delta\lambda_i \tag{17}$$

where $\Delta\lambda_i$ is the interval between the two neighboring values λ_i.

2.6. Calculations of cell parameters

To calculate the solar cell efficiency and output power density, many parameters such as; open-circuit voltage; maximum current density and maximum voltage must be firstly known. These parameters can be estimated from an illuminated J–V characteristic curve which can be presented in the form:

$$J(V) = J_d - J_{ph} \tag{18}$$

where J_d is the dark current density and J_{ph} is the photocurrent density.

In most papers, the analytical description of J–V characteristics have been done using a semi-empirical formula for the dark current density in the so-called "ideal" solar cell which is described by the Shockley equation:

$$J_d(V) = J_S\left[\exp\left(\frac{qV}{kT}\right) - 1\right] \tag{19}$$

where J_s is the saturation current density equals the reverse current independent on the voltage V as qV is higher than a few kT. In this work, the measured J–V characteristics of CdS/PbS heterostructure are governed by the generation–recombination Sah–Noyce–Shockley theory. The Sah–Noyce–Shockley theory supposes that the generation–recombination rate in the section x of the space-charge region is determined by expression (Sah et al., 1957):

$$U(x,V) = \frac{n(x,V)P(x,V) - n_i^2}{\tau_{Po}[n(x,V) + n_1] + \tau_{no}[P(x,V) + P_1]} \tag{20}$$

where τ_{no} and τ_{po} is the effective lifetime of electrons and holes in the depletion region, respectively, n_i is the intrinsic carrier concentration and the values n_1 and P_1 are determined by the energy spacing between the top of the valence band and the generation–recombination level E_t, i.e.

$$P_1 = N_v \exp(-(E_t/kT) \tag{21}$$

$$n_1 = N_c \exp(-(E_g - E_t)/kT) \tag{22}$$

where N_c and N_v is the effective state densities in the conduction and valence bands, respectively and given by:

$$N_c = 2\left(\frac{m_n KT}{h^2}\right)^{3/2}, \quad N_v = 2\left(\frac{m_p KT}{h^2}\right)^{3/2} \tag{23}$$

In this equation, m_n and m_p are the effective masses of electrons and holes.

The values $n(x, V)$ and $P(x, V)$ in Eq. (20) are the carrier concentration in the conduction and valence bands and given by Kosyachenko et al. (2007).

$$P(x,V) = N_c \exp\left[-\frac{\Delta\mu + \varphi(x,V)}{kT}\right] \tag{24}$$

$$n(x,V) = N_v \exp\left[-\frac{E_g - \Delta\mu - \varphi(x,V) - qV}{kT}\right] \tag{25}$$

where $\Delta\mu$ is the energy spacing between the Fermi level and the top of the valence band of CdTe and $\varphi(x, V)$ is the electron energy in the space charge region is given by:

$$\varphi(x,V) = (\varphi_0 - qV)\left(1 - \frac{x}{W}\right) \tag{26}$$

According to the Eqs. (20)–(26), the recombination-generation current are found by integration of $U(x, V)$ throughout the entire depletion layer (Kosyachenko et al., 2009):

$$J_{gr} = q\int_0^W U(x,V)dx \tag{27}$$

On the other hand, since in CdS/CdTe junction the barrier for holes is higher than that for electrons, the electron component dominates the over-barrier current. Obviously, the electron flow current in analogous to that occurring in the p–n junction and one can write for the over-barrier current density (Sze, 1981):

$$J_n == q\frac{n_p L_n}{\tau_n}\left[\exp\left(\frac{qV}{kT}\right) - 1\right] \tag{28}$$

where n_p is the concentration of electrons in the bulk part of the p-CdTe layer, given by:

$$n_P = N_c \exp\left(-\frac{E_g - \Delta\mu}{kT}\right) \tag{29}$$

Thus, according to the above-presented, the dark current density $J_d(V)$ is the sum of the generation–recombination and over-barrier components:

$$J_d(V) = J_{gr}(V) + J_n(V) \tag{30}$$

The CdS/PbS solar cell efficiency can be expressed by:

$$\eta = \frac{FF \times J_{SC} \times V_0}{P_{in}} \tag{31}$$

where FF is the fill factor, V_0 is the open circuit voltage, P_{in} is the density of the total AM 1.5 solar radiation power (equals 96.3 mW/cm^2) (Toshifumi et al., 1993).

In this work, the efficiency of thin film solar cell based on PbS is compared with the Shockley–Queisser limit that refers to the calculation of the maximum theoretical efficiency of a solar cell made from a single pn junction. The dependence of this efficiency on the band gap energy (E_g) of the used absorber layer is given by the following expression (Shockley and Queisser, 1961):

$$U(E_g) = \frac{E_g Q_S}{P_S} \tag{32}$$

where Q_S is the number of absorbed photons ($E < E_g$) per unit area, per unit time and P_S is the solar power per unit area. This calculation assumed an idealized device so the practical limits are even smaller. The main assumptions are that all incident photons are captured, all above-band-gap photons are absorbed, complete thermalization occurs, the transport and collection of charges are lossless, and that only radiative or Auger recombination occurs.

The fill factor can be written as:

$$FF = \frac{P_m = J_m \times V_m}{J_{SC} \times V_0} \tag{33}$$

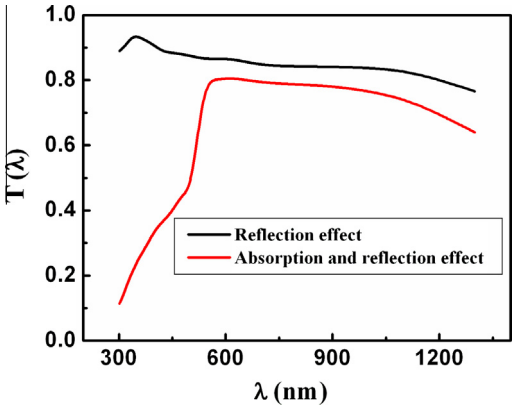

Fig. 2. Calculated transmission spectrum $T(\lambda)$ due to reflection from all layers and absorption in ITO and CdS layer.

where J_m and V_m are the maximum current density and voltage, respectively.

3. Results and discussion

Using Eqs. (4) and (5), the transmission spectrum $T(\lambda)$ that reaches the effective layer is calculated and plotted in Fig. 2. The data of refractive index and extinction coefficient of ITO, CdS and PbS are taken from (http://homepages.rpi.edu/schubert/Educational-resources/Materials-Refractive-index-and-extinction-coefficient.pdfS). The extinction coefficient of glass substrate is assumed to be equal zero, while its refractive index is calculated using Sellmeier dispersion equation (Kasap, 2000). It is clear that, the transmission spectrum due to multi reflections effect records value of 0.92–0.77 in the wavelength range of 600–1300 nm. When the absorption effect is taken into calculations, the transmission spectrum decreases comparing with the above case and records value of 0.8–0.67 in the wavelength range 550–1300 nm. At low wavelength, the optical losses record high value of about 88% at $\lambda = 300$ nm and about 50% at $\lambda = 500$ indicating that the big part of optical losses in the wavelength range 300–550 nm is due to the absorption. This result shows that $T(\lambda)$ is less than unity due to reflection and absorption losses. These losses are ranged from 20% to 33% in the wavelength range of 550–1300 nm. This optical losses will affect in the calculation of short-circuit current density and in the efficiency of CdS/PbS solar cell.

In above results, the thickness of both ITO layer and CdS layer are 100 nm. It is expected that by thinning the thickness of ITO layer and/or CdS layer it is possible to reduce the optical losses due to decreasing the absorption losses. It is known, however, that it is difficult to obtain uniform and pin-hole free CdS layers thinner than ~50 nm.

Dependence of absorptivity of solar radiation power on the thickness of PbS layer (d_{PbS}) under condition of AM1.5 solar irradiation (ISO 9845-1:1992) is shown in Fig. 3. It is clear that the PbS thickness of 20–30 μm is sufficient to absorb more than 99% from the incident solar radiation.

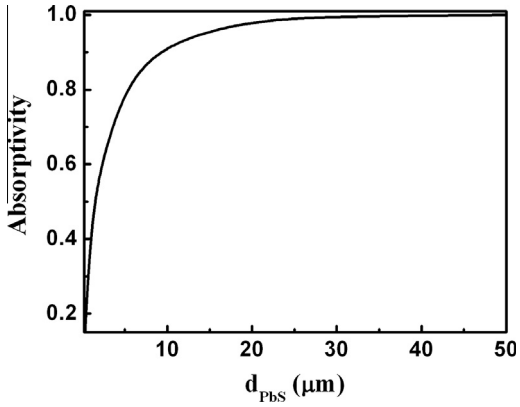

Fig. 3. Dependence of absorptivity of solar radiation power on thickness of the PbS layer (d_{PbS}) under condition of AM1.5 solar radiation.

At thickness 2 μm, the capacity of absorptivity is about 60%. The current calculations ignore the effect of the metallic back contact. Using the effect of metallic back contact will increase the absorptivity in the absorber layer and hence its thickness can be reduced without decreasing the amount of absorptivity. It is reported (Kosyachenko et al., 2013) if the reflectance from the back contact is 100% the absorptivity will be as same as the case of using a double thickness of the absorber layer. As concluded from Fig. 3, a thickness of about 15 μm will absorb more than 95% of photons without taking into account the effect of back contact.

In the calculations of internal quantum efficiency, we assumed that the absorption coefficient of the effective layer (PbS) is independent on its thickness. Thus according to Eqs. (8) and (9), the drift component of internal quantum efficiency is dependent on the width of the ablation layer and the diffusion component is dependent on the width of space charge region as well as on the thickness of PbS layer. Fig. 4 represents the dependence of η_{drift} on the width of space charge region (W). The calculations are carried out at $S = 10^7$ cm/s (Fig. 4a) and at $S = 0$ (Fig. 4b). The present width of space charge region 0.13–12 μm corresponds to the concentration of $N_a - N_d$ in the range of 10^{17}–10^{13} cm^{-3}. Fig. 4a shows that η_{drift} decreases with increasing wavelength and decreasing the width of space charge region. The decreasing of η_{drift} with wavelength is due to decreasing of α with wavelength. With narrowing the barrier region from 12 μm to 0.13 μm (increasing $N_a - N_d$ from 10^{13} cm^{-3} to 10^{17} cm^{-3}), the value of η_{drift} decreases due to a large portion of photons is absorbed outside the space-charge region. When $S = 0$ as shown in Fig. 4b, η_{drift} is close to 1 at lower wavelength and wide width of space charge region.

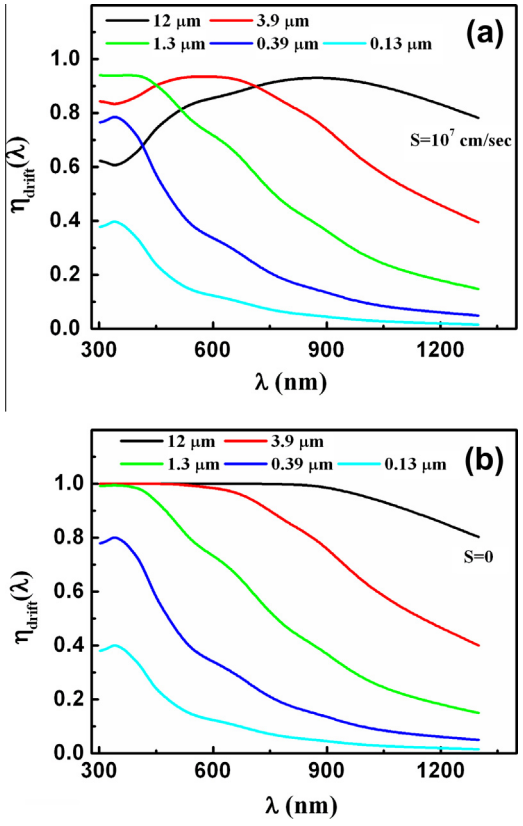

Fig. 4. Drift component of internal quantum efficiency (η_{drift}) as a function of wavelength at different values of space charge region width (W) at front surface recombination velocity $S = 10^7$ cm/s (a) and $S = 0$ (b).

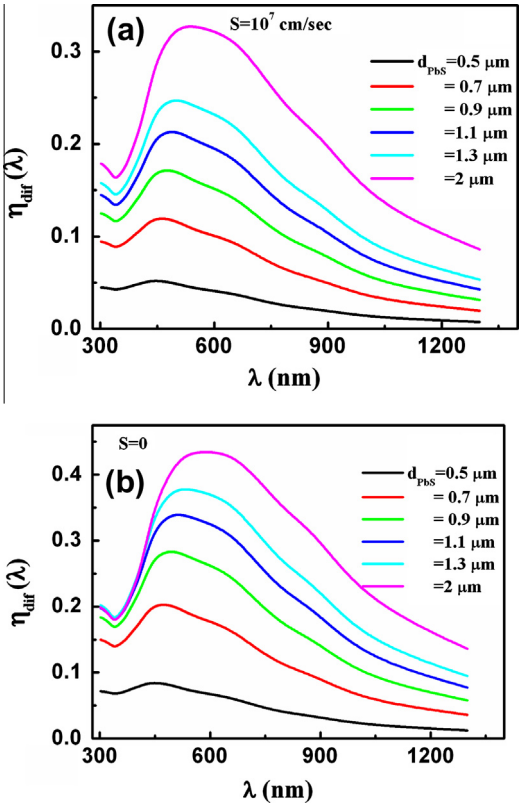

Fig. 5. Diffusion component of internal quantum efficiency (η_{dif}) as a function of wavelength at different values of PbS thickness (d_{PbS}) at front surface recombination velocity $S = 10^7$ cm/s (a) and $S = 0$ (b).

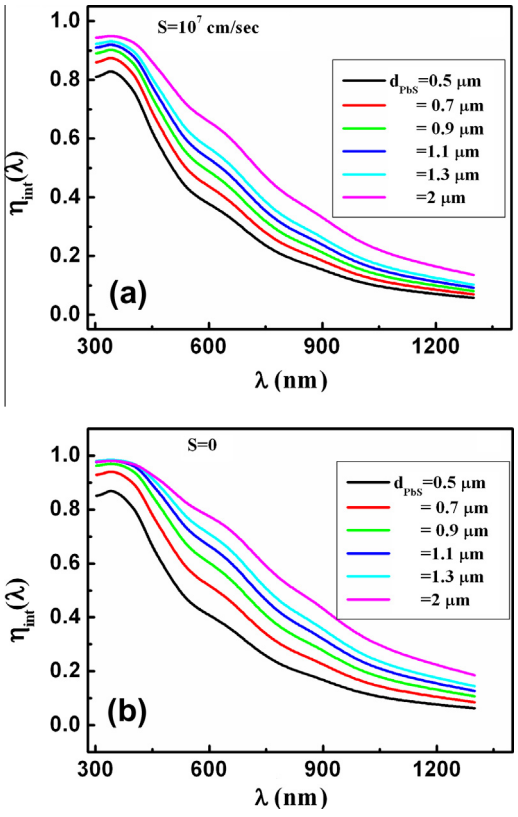

Fig. 6. Internal spectral quantum efficiency (η_{int}) at different values of PbS thickness (d_{PbS}) at front surface recombination velocity $S = 10^7$ cm/s (a) and $S = 0$ (b).

The second component (η_{dif}) of internal quantum efficiency as a function of wavelength at different values of PbS thickness and at $W = 0.39$ μm is plotted in Fig. 5. It is clear that the maximum η_{dif} is observed at thicker PbS and at $S = 0$. Besides, the values of $\eta_{dif} < \eta_{drift}$ which means that the contribution of diffusion component of quantum efficiency is small comparing with the contribution of drift component.

The total internal quantum efficiency (η_{int}) as a function of wavelength at different values of PbS thickness and at $W = 0.39$ μm is shown in Fig. 6. From this figure we can see that the recombination losses (front + back) take place in all values of wavelength and thickness of PbS layer, since $\eta_{int} < 1$ in all cases. The average of η_{int} in all wavelength range ($\lambda = 300$–1300 nm) for $d_{PbS} = 0.5$ μm and 2 μm is about 0.5 and 0.65, respectively.

Fig. 7 shows the charge collection efficiency (η_c) computed by Eq. (16) for electron lifetimes of 10^{-9} s. It is clear that η_c increases with increase the value of x (which is measured from PbS side) and attains to saturation case when x is close to the width of space-charge region (W). The recombination losses in space-charge region are about 82% at $x = 0$ and it decrease strongly with increase x reaching to about 1.5% at $x = W$. That indicates, the recombination losses in space-charge region can be ignored at narrowing width of space-charge region.

Calculating the short-circuit current density gives a quantitative description of losses caused by reflection from different layers in CdS/PbS cell, absorption in ITO and CdS layers and recombination losses at the front and back surfaces of PbS layer. Using Eq. (17), the dependence of short-circuit current density of CdS/PbS heterostructure on the thickness of the effective layer is calculated under the conditions of AM1.5 (96.3 W/cm^2) solar irradiation and plotted in Fig. 8. Calculations were made for the surface recombination velocities of $S = 10^7$ cm/s and $S = 0$. The width of space charge region is assumed to be 0.39 μm which corresponds to $N_a - N_d = 10^{16}$ cm^{-3}. In order to estimate the quantitative optical and recombination losses, we put $T(\lambda) = 1$ and $\eta_{int}(\lambda) = 1$ in Eq. (17) to obtain the maximum short-circuit current density of $J^0_{SC} = 41$ mA/cm^2 for $S = 10^7$ cm/s. When both the optical and recombination losses are taken into calculations, it is found that $J_{SC} = 7.28$ mA/cm^2 for $d_{PbS} = 0.5$ μm and 13.2 mA/cm^2 for $d_{PbS} = 2$ μm. This indicates that the optical and recombination losses are about 82% and 67% at $d_{PbS} = 0.5$ μm and 2 μm, respectively. Moreover, the results from Fig. 2 show that the optical losses are about 30%, therefore the recombination losses are in the range of 35–50 depending on the thickness of effective layer and these results confirm the results obtained from Fig. 6.

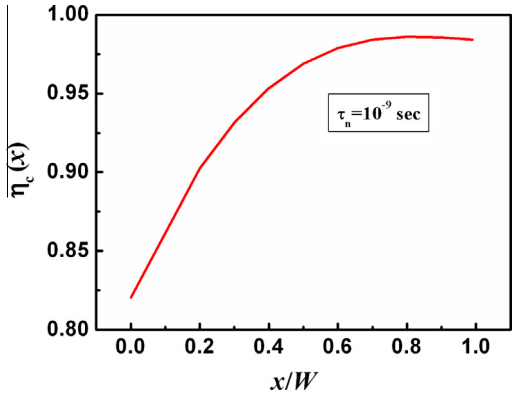

Fig. 7. The coordinate dependences of the charge-collection efficiency η_c calculated for electron lifetimes τ_n of 10^{-9} s.

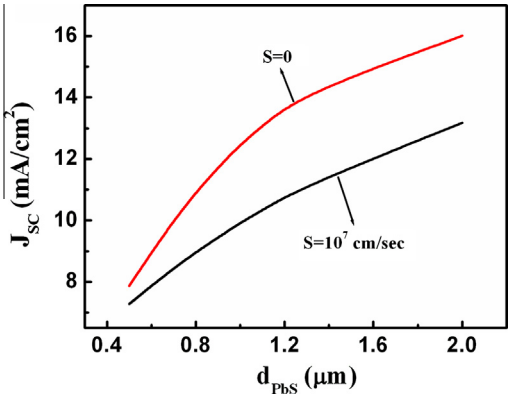

Fig. 8. Dependence of short-circuit current density (J_{SC}) on the thickness of absorber layer (d_{PbS}) at front surface recombination velocity $S = 10^7$ cm/s and $S = 0$.

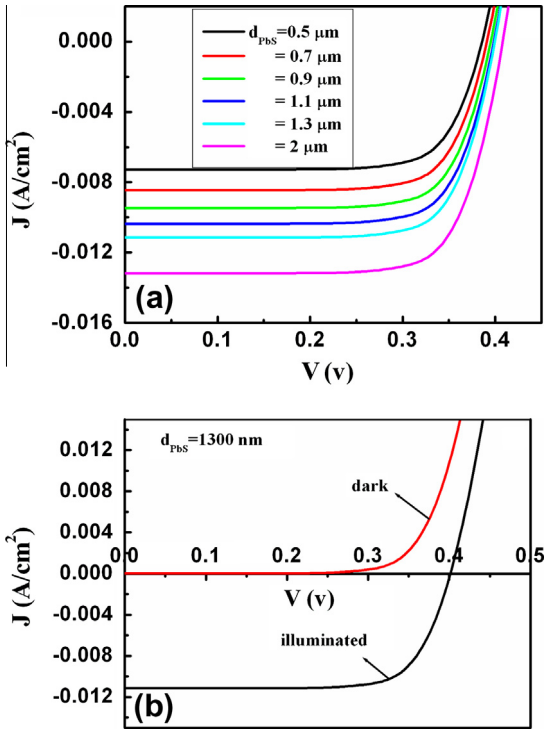

Fig. 9. J–V characteristic curve of CdS/PbS solar cell under illumination at various thicknesses of absorber layer (a) and the comparing between dark and illuminated current when the thickness of PbS is 1300 nm (b).

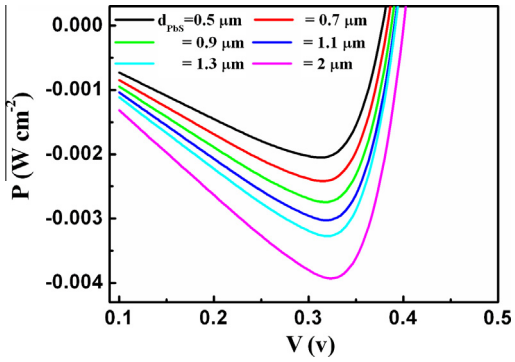

Fig. 10. The output power density (P) as a function of applied voltage (V) at different thicknesses of the absorber layer of CdS/PbS solar cell.

When the velocity of front surface recombination is reduced to zero, the values of J_{SC} increase and hence the recombination losses decrease. In later case, the short-circuit current density records value of $J_{SC} = 7.86$ mA/cm^2 and 16 mA/cm^2 for $d_{PbS} = 0.5$ μm and 2 μm, respectively. Then, the optical and recombination losses of this case are about 80% and 61%, respectively.

Fig. 9 shows J–V characteristics of thin film CdS/PbS solar cells at different thicknesses of PbS layer under the illumination condition of AM1.5 solar irradiation. It is clear from Fig. 9a that the illumination becomes more significant on CdS/PbS cell as the thickness of absorber is increasing. Fig. 9b compares between the dark and illuminated current of CdS/PbS solar cell at $d_{PbS} = 1300$ nm. From this figure and using Eqs. (31) and (33), some important parameters such as V_0, V_m, J_m, FF, P_m and η are estimated and listed in Table 2 as a function of PbS thickness. We can observe that, all these parameters expect FF increase with increasing the absorber thickness. The trend of the fill factor FF is weakly depending on the thickness of absorber layer. Firstly, it decreases slightly with thickness from 72% to 70% and then starts to increase slightly with thickness to attain 72.8 at the highest thickness. Apart from the values of FF at PbS thickness range 700–900 nm, FF seems to be constant with average value of 72%. That indicate the capacity of the device to collect the charge carriers is approximately constant for various thickness of the absorber layer. The minimum cell efficiency of 2.16% is observed at $d_{PbS} = 0.5$ μm, while the maximum efficiency is 4.13% is observed at $d_{PbS} = 2$ μm. These values of efficiency are considered greater than the efficiency that estimated in some previous work (Bhandari et al., 2013; Hernandez-Borja et al., 2011; Obaid et al., 2012, 2013a,b). This difference in efficiencies between this work and the previous work maybe due to that this work is based on some assumptions such as, the value of electron lifetime, the value of electron diffusion coefficient, the value of velocity of surface recombination as well as the thickness that used here (particular 2 μm) is considered higher than the used thickness in these previous work.

Moreover, comparing the current efficiency with Shockley–Queisser limit with applying the same assumption in Eq. (32) to PbS solar cells, the estimated upper limit reaches about 15% efficiency, which is almost three times the current highest efficiency achieved. The big difference between Shockley–Queisser and the current efficiency is mainly due to the optical and recombination losses.

The output power density of CdS/PbS solar cells as a function of applied voltage is shown in Fig. 10 at different thicknesses of absorber layer. It can be seen that the maximum power is observed at applied voltage of 0.34 V and with increasing the thickness of absorber layer the power

Table 2
The maximum current density (J_m), maximum voltage (V_m), open circuit voltage (V_0), fill factor (FF), output power density (P_{out}) and efficiency (η) of thin film CdS/PbS solar cells at different values of thickness of the effective layer (PbS).

d_{PbS} (nm)	J_m (A/cm^2)	V_m (V)	V_0 (V)	FF (%)	P_{out} (mW/cm^2)	η (%)
500	0.0064	0.325	0.394	72.5	2.076	2.16
700	0.0071	0.336	0.398	70.9	2.38	2.47
900	0.0077	0.345	0.402	69.8	2.66	2.76
1100	0.0089	0.338	0.405	71.6	2.99	3.11
1300	0.0100	0.328	0.406	72.5	3.30	3.42
2000	0.0125	0.318	0.414	72.8	3.98	4.13

increases. This is due to increasing the cell efficiency with thickness as shown in Fig. 9 and Table 2.

4. Conclusions

Many parameters such as; internal quantum efficiency, short-circuit current density, open circuit voltage, fill factor, output power density and efficiency of a thin film solar cell with structure ITO/CdS/PbS were studied theoretically in this work. The absorption in ITO and CdS layer as well as multi-reflections from different layers were taken into account in the calculating the transmission spectrum. The dependence of drift and diffusion components of spectral quantum efficiency on the width of depletion layer and on the thickness of absorber layer was studied at two values of velocity of surface recombination. The J–V characteristic curve under illumination condition was studied to estimate some important parameters such as open circuit voltage, maximum current density and maximum voltage.

The obtained results showed that:

(1) The short-circuit current density was about 7.28 mA/cm^2 at thickness 0.5 μm of the absorber layer and increased up to 16 mA/cm^2 with further increase in the thickness up to 2 μm.
(2) The open circuit voltage, maximum current density, maximum voltage, output power density and efficiency of CdS/PbS solar cell increased with increasing the absorber layer thickness.
(3) The fill factor represented weak dependence on the thickness of absorber layer and recorded an average value of about 72%.
(4) The maximum cell efficiency of 4.13% was achieved at $d_{ITO} = 100$ nm, $d_{CdS} = 100$ nm, $d_{PbS} = 2$ μm, $S = 10^7$ cm/s, $W = 0.39$ μm and $\tau = 10^{-9}$ s.

Acknowledgment

The author would like to thank the Deanship of scientific research, King Saud University, Riyadh, Saudi Arabia, for funding and supporting this research.

References

Akhtar, J., Malik, M.A., Brien, P.O., Wijayantha, K.G.U., Dharmadasa, R., Hardman, S.J.O., Graham, D.M., Spencer, B.F., Stubbs, S.K., Flavell, W.R., Binks, D.J., Sirotti, F., El Kazzie, M., Silly, M., 2010. A greener route to photoelectrochemically active PbS nanoparticles. J. Mater. Chem. 20, 2336–2344.

Bhandari, K.P., Roland, P.J., Mahabaduge, H., Haugen, N.O., Grice, C.R., Jeong, S., Dykstra, T., Gao, J., Ellingson, R.J., 2013. Thin film solar cells based on the heterojunction of colloidal PbS quantum dots with CdS. Sol. Energy Mater. Sol. Cells 117, 476–482.

Gao, J., Perkins, C.L., Luther, J.M., Hanna, M.C., Chen, H.-Y., Semonin, O.E., Nozik, A.J., Ellingson, R.J., Beard, M.C., 2011. N-Type transition metal oxide as a hole extraction layer in PbS quantum dot solar cells. Nano Lett. 11, 3263–3266.

Gertman, R., Osherov, A., Golan, Y., Fisher, I.V., 2014. Chemical bath deposited PbS thin films on ZnO nanowires for photovoltaic applications. Thin Solid Films 550, 149–155.

Green, M.A., Emery, K., Hishikawa, Y., Warta, W., Dunlop, E.D., 2013. Solar cell efficiency tables (version 41). Prog. Photovoltaics: Res. Appl. 21, 1–11.

Hecht, K.Z., 1932. Physics 77, 235.

Hernandez-Borja, J., Vorobiev, Y.V., Ramırez-Bon, R., 2011. Thin film solar cells of CdS/PbS chemically deposited by an ammonia-free process. Sol. Energy Mater. Sol. Cells 95, 1882–1888.

Ip, A.H., Thon, S.M., Hoogland, S., Voznyy, O., Zhitomirsky, D., Debnath, R., Levina, L., Rollny, L.R., Carey, G.H., Fischer, A., Kemp, K.W., Kramer, I.J., Ning, Z., Labelle, A.J., Chou, K.W., Amassian, A., Sargent, E.H., 2012. Hybrid passivated colloidal quantum dot solids. Nat. Nano 7, 577–582.

Kramer, I.J., Sargent, E.H., 2011. Colloidal quantum dot photovoltaic:a path forward. ACS Nano 5, 8506–8514.

Kasap, S.O., 2000. Optoelectronics and Photonics: Principles and Practice. Prentice-Hall, New Jersey.

Kosyachenko, L.A., Sklyarchuk, V.M., Sklyarchuk, O.F., Gnatyuk, V.A., 2007. Features of the generation–recombination processes in CdTe-based Schottky diodes. Semicond. Sci. Technol. 22, 911–918.

Kosyachenko, L.A., Savchuk, A.I., Grushko, E.V., 2009. Dependence of efficiency of thin-film CdS/CdTe solar cell on parameters of absorber layer and barrier structure. Thin Solid Films 517, 2386–2391.

Kosyachenko, L.A., Mathew, X., Roshko, V.Y., Grushko, E.V., 2013. Optical absorptivity and recombination losses: the limitations imposed by the thickness of absorber layer in CdS/CdTe solar cells. Sol. Energy Mater. Sol. Cells 114, 179–185.

Kosyachenko, L.A., Grushko, E.V., Motushchuk, V.V., 2006. Recombination losses in thin-film CdS/CdTe photovoltaic devices. Sol. Energy Mater. Sol. Cells 90, 2201–2212.

Mohamed, H.A., Hadia, N.M.A., 2013. Improvement in the efficiency of thin film CdS/CdTe solar cells using different TCO materials. In: International Congress on Energy Efficiency and Energy Related Materials, Antalya, Turkey, p. 24.

Mohamed, H.A., 2013. Dependence of efficiency of thin-film CdS/CdTe solar cell on optical and recombination losses. J. Appl. Phys. 113, 093105.

Nair, G., Chang, L.Y., Geyer, S.M., Bawendi, M.G., 2011. Perspective on the prospects of carrier multiplication nanocrystal solar cell. Nano Lett. 11, 2145–2151.

Nozik, A.J., 2002. Quantum dot solar cells. Phys. E: Low-Dimensional Syst. Nanostruct. 14, 115–120.

Obaid, A.S., Mahdi, M.A., Hassan, Z., Bououdin, M., 2012. Preparation of chemically deposited thin films of CdS/PbS solar cell. Superlattice. Microst. 52, 816–823.

Obaid, A.S., Hassan, Z., Mahdi, M.A., Bououdin, M., 2013a. Fabrication and characterisations of n-CdS/p-PbS heterojunction solar cells using microwave-assisted chemical bath deposition. Sol. Energy 89, 143–151.

Obaid, A.S., Mahdi, M.A., Hassan, Z., Bououdin, M., 2013b. PbS nanocrystal solar cells fabricated using microwave-assisted chemical bath deposition. Int. J. Hydrogen Energy 38, 807–815.

Sah, C., Noyce, R., Shokley, W., 1957. Carrier generation and recombination in p–n junctions and p–n junction characteristics. Proc. IRE 45, 1228–1243.

Sambur, J.B., Novet, T., Parkinson, B.A., 2010. Multiple exciton collection in a sensitized photovoltaic system. Science 330, 63–66.

Semonin, O.E., Luther, J.M., Choi, S., Chen, H.Y., Gao, J., Nozik, A.J., Beard, M.C., 2011. Peak external photocurrent quantum efficiency exceeding 100% via MEG in a quantum dot solar cell. Science 334, 1530–1533.

Shockley, W., Queisser, H.J., 1961. Detailed balance limit of efficiency of p–n junction solar cells. J. Appl. Phys. 32, 510–519.

Smith, D.K., Luther, J.M., Semonin, O.E., Nozik, A.J., Beard, M.C., 2011. Tuning the synthesis of ternary lead chalcogenide quantum dots by balancing precursor reactivity. ACS Nano 5, 183–190.

Sze, S., 1981. Physics of Semiconductor Devices, second ed. Wiley, New York.
Sze, S.M., Kwok, K.N.G., 2007. Physics of Semiconductor Devices. Wiley, New Jersy.
Toshifumi, T., Adachi, S., Nakanishi, H., Ohtsuka, K., 1993. Optical constants of $Zn_{1-x}Cd_xTe$ ternary alloys: experiment and modeling. Jpn. Appl. Phys. 32, 3496–3501.
Velizhanin, K.A., Piryatinski, A., 2011. Numerical study of carrier multiplication pathways in photoexcited nanocrystal and bulk forms of PbSe. Phys. Rev. Lett. 106, 207401–207404.
Yang, W.J., Ma, Z.Q., Tang, X., Feng, C.B., Zhao, W.G., Shi, P.P., 2008. Internal quantum efficiency for solar cells. Sol. Energy 82, 106–110.
Wise, F.W., 2000. Lead salt quantum dots: the limit of strong quantum confinement. Acc. Chem. Res. 33, 773–780.